

Nano size TiC reinforced iron aluminide cermets made by mechanical alloying

Se-Hyun Ko*, Wonsik Lee, Jin-Man Jang, Bermha Cha and Jung-Sik Seo

Production R&D Department, Korea Institute of Industrial Technology, Incheon 406-840, Korea

TiC/Fe-Al cermets were produced by the mechanical alloying and sintering process. The composition of the binder phase was designed to be Fe-28 at%Al with TiC of 50, 70 and 90 vol %. Mechanical alloying of elemental powders of Ti, C, Fe and Al promoted the formation of the supersaturated TiC solid solution containing Fe and Al. During sintering Fe₃Al phase precipitated from the supersaturated TiC solid solution. Relative densities of sintered bodies were in the range from 98.3% to 95.1% as the volume fraction of TiC increased from 50% to 90%. Microstructures of sintered bodies containing TiC of 50 vol% and 70 vol% were consisted of three regions; 1-2 μm TiC particles, Fe₃Al binder with 100 nm TiC particles and particle-free Fe₃Al regions. And the sintered body containing 90 vol% TiC was consisted of two regions of TiC and particle-free Fe₃Al. Indentation test results showed that Fe₃Al with 100 nm size TiC particles and particle-free Fe₃Al regions are effective for the prevention of crack propagation. The bending strength of 50 vol% and 70 vol% TiC/ Fe₃Al cermets was higher than 1700 MPa.

Key words: In-situ cermet, Titanium carbide, Iron aluminide, Mechanical alloying, Bending strength.

Introduction

As a promising candidate for a structural material, iron aluminides have been studied by many researchers. This is because the iron aluminides have many attractive properties such as low density, relatively low production cost, excellent oxidation and corrosion resistance as well as high temperature strength [1, 2]. It has been also found that the iron aluminides have an acceptable ductility and fracture toughness as compared to many ordered intermetallic alloys [2, 3]. From these merits, iron aluminides have been investigated as binders for fabricating ceramic/iron aluminide composites by pressureless melt infiltration [4-6].

Titanium carbide (TiC) possesses excellent properties such as high hardness, high Young's modulus, low density and low chemical reactivity and therefore has been found to be a suitable reinforcing material for wear and high temperature applications [5]. Especially, TiC reinforced cermets have been considered as potential materials to overcome the shortcomings of WC/Co such as poor oxidation, corrosion resistance, high density, high cost and environmental toxicity [6]. Subramanian et al. [7] have reported that Fe-40 at%Al/TiC cermets with 60, 70 and 80 vol% TiC prepared by a melt infiltration exhibited 1058, 1034 and 750 MPa of three-point bending strength, respectively. Although the values of strength are high enough for static wear applications in corrosive atmosphere,

subsequent improvements on strength are needed in some cases such as a heavy-duty cutting, etc. [6]. Another problem in manufacturing Fe-40 at%Al/TiC cermets by pressureless melt infiltration was that Fe-40 at%Al/TiC cermets with over 85 vol% TiC have too much defect to determine the mechanical properties [8].

Many kinds of alloys and composites were produced by a mechanical alloying technique which was developed in 1966 [9]. This technique can also achieve nanocrystals, reactive milling synthesis and intermetallic compounds as well as alloying at the atomic level. Mechanical alloying and sintering process have the advantages that volume fraction of reinforcement can be easily controlled and near-net shape production is possible. Furthermore, a solid state sintering after mechanical alloying allows the reinforcement to be in fine distribution, which generally increase the strength of composites.

In our previous works [10, 11], in-situ Fe-28 at%Al/TiC composites with 16 vol% TiC were successfully manufactured by melting or mechanical alloying-sintering processes [10, 11]. TiC particles, which were produced by in-situ reaction during mechanical alloying-sintering process, were submicron sized and uniformly distributed in the Fe-28 at%Al matrix. This work aims to produce the TiC/Fe-28 at%Al cermets with 50 ~ 90 vol% TiC by in-situ reaction of elemental powders. The microstructural evolution, mechanical properties and manufacturing process were discussed in details.

Experimental Procedure

In-situ cermets of TiC/Fe-Al were manufactured by mechanical alloying-pulse discharge sintering process.

*Corresponding author:
Tel : +82-32-850-0219
Fax: +82-32-850-0430
E-mail: shko@kitech.re.kr

The raw materials were 99.9 wt% titanium powder of 10 μm , 99.9 wt% graphite powder of 5 μm , 99 wt% iron powder of 5 μm and 99.9 wt% aluminum powder of 10 μm . Fe-28 at%Al was selected as a matrix composition. The cermets were formulated to contain 50%, 70% and 90% volume of TiC. The designations and chemical compositions of the cermets are summarized in Table 1. A ratio of titanium to carbon was 51.6 : 48.4, which was determined in the earlier experiment [10].

Mechanical alloying of elemental powders was carried out in a vibratory ball mill. Powders, together with chrome steel balls of 25.4 mm diameter, were sealed into cylindrical stainless steel vials in a high purity argon filled glove box in order to minimize the oxygen contamination. After milling of 200 hours, the milled powders were sintered using a pulse discharge sintering. The sintering temperatures of the FA-50TiC, FA-70TiC and FA-90TiC were 1150 $^{\circ}\text{C}$, 1200 $^{\circ}\text{C}$ and 1250 $^{\circ}\text{C}$, respectively. A heating rate was 20 $^{\circ}\text{C}/\text{minute}$ and holding time at given temperatures was 20 minutes. The milled powders were filled in a graphite mold and were pressed by two graphite punches at both ends. A constant pressure of 55 MPa was applied during sintering.

Characterization of the milled powders and sintered bodies was carried out by X-ray diffraction (XRD). The sintered bodies were examined metallographically using a scanning electron microscope equipped with energy dispersive X-ray spectrometer (SEM-EDX). In addition, the binder of surface on each sample was partially etched away to observe the shape of TiC. The samples were put into an HCl + H₂O (1 : 1) solution at room temperature for 2 minutes to dissolve the binder of surface. The densities of the sintered cermets were measured by Archimedes' method. The samples were machined and polished using diamond slurry to 10 mm \times 5 mm \times 25 mm with a span of 20 mm for the three point bending test. Bending tests were performed at room temperature. The cross-head-speed was 0.5 mm/min. Two specimens were tested for each cermet. Vickers indentation test was carried out at loads of 9.8, 49, 98 and 196 N. For each load at least five indentations were made and the average indentation size

and crack length were evaluated.

Results and Discussion

The XRD patterns of the milled powders and sintered bodies are presented in Fig. 1. TiC peaks appeared in all the milled powders, indicating that TiC was synthesized during mechanical alloying. It was reported that TiC powder can be synthesized by a solid-state reaction during mechanical milling of elemental powders [12, 13]. The grain size of the TiC powders after an optimized milling was under 20 nm. It was also found that the peaks of iron and aluminum disappeared after milling of 200 hours caused by the solid solution. In the TiC-Fe-Al system, TiC phase have very low solubility limit for Fe and Al up to high temperature [5]. An extension of solid solubility as well as an alloying in immiscible systems has been

Table 1. Designations and chemical compositions of cermets.

Designation	Nominal Composition	Amounts of elemental addition [at% (wt%)]			
		Ti	C	Fe	Al
FA-50TiC	(Fe-28 at%Al)- 50 vol%TiC	28.0 (34.8)	26.2 (8.2)	33.0 (48.0)	12.8 (9.0)
FA-70TiC	(Fe-28 at%Al)- 70 vol%TiC	37.9 (51.6)	35.5 (12.2)	19.2 (30.5)	7.4 (5.7)
FA-90TiC	(Fe-28 at%Al)- 90 vol%TiC	47.2 (70.7)	44.3 (16.6)	6.1 (10.7)	2.4 (2.0)

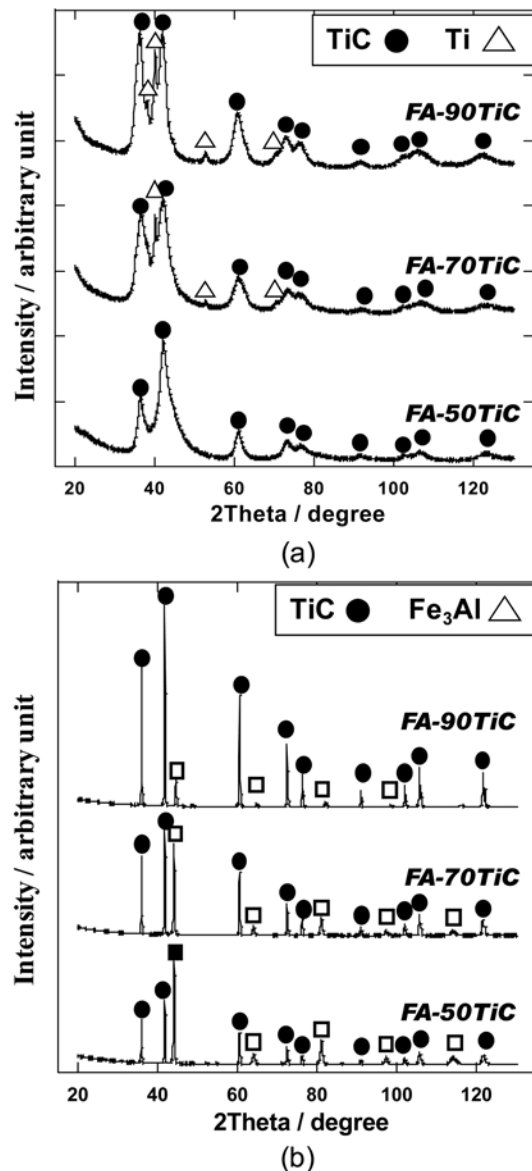


Fig. 1. XRD patterns of (a) milled powders and (b) sintered bodies.

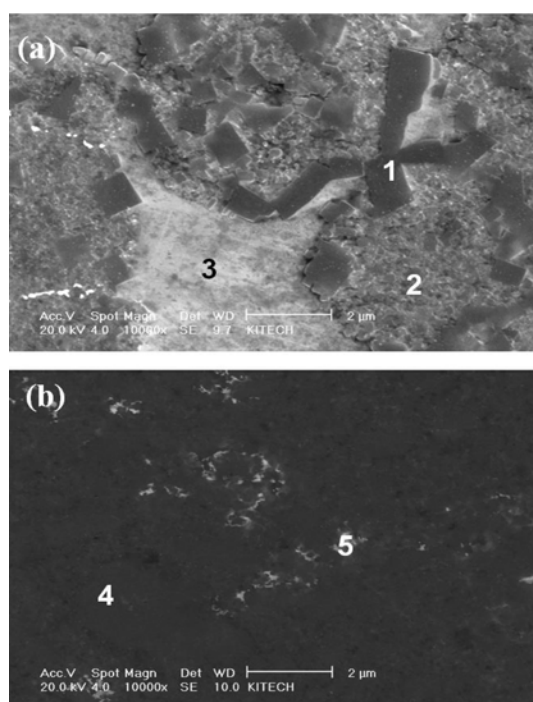
reported on mechanical alloying of many systems. Additionally, it is seen that the peak broadening occurs in all the milled powders. The broadening of TiC peaks is thought to be due to the refinement of the crystalline size and lattice distortion by the solid solution and severe deformation. All the sintered samples exhibited XRD peaks of TiC and Fe₃Al peaks only [Fig. 1(b)]. On the basis of the peak intensity on the milled powders and sintered bodies, it is clear that TiC phase was almost formed during milling and the precipitation of Fe₃Al from the supersaturated TiC was completed during sintering process. In addition, any free element such as Ti, C, Fe and Al was not detected after sintering, while free Ti was detected after milling in the FA-70TiC and FA-90TiC.

The surfaces of sintered bodies were polished and the densities were measured by the Archimedes' method. The densities of the FA-50TiC, FA-70TiC and FA-90TiC were measured to be 5.631 g/cm³, 5.258 g/cm³ and 4.839 g/cm³, respectively. The relative densities were calculated from the nominal density derived by the rule of mixtures and measured density. The relative

densities of the FA-50TiC, FA-70TiC and FA-90TiC were 98.3%, 97.2% and 95.1%, respectively. The decrease of relative density with the increase of TiC vol% was attributed to the increase of micro-porosity.

Fig. 2 shows SEM micrographs and EDX results of the FA-50TiC and FA-70TiC. It is revealed that the FA-50TiC was consisted of micro size TiC particles (Position 1), nano size TiC particles with Fe₃Al binder (Position 2), and TiC-free Fe₃Al region (Position 3). Earlier study [11] on in-situ Fe₃Al/TiC composite containing 16 vol% TiC showed the similar microstructure, while the size of the area at each phase and the particles size were different. It was reported that the the presence of larger TiC particles was due to an insufficient milling time. The insufficient alloying of the milled powders left the Ti-rich phase in the milled powders and therefore large TiC particles were formed in the regions of Ti-rich phase during sintering. Although the microstructure of the FA-70TiC is similar to that of the FA-50TiC, the FA-90TiC contains two regions of TiC (Position 4) and Fe₃Al (Position 5).

In order to observe the morphology of TiC particles in detail, the binder phase of cermets, Fe₃Al, was partially removed by the chemical deep etching. Fig. 3 shows SEM micrographs of the FA-50TiC and FA-90-TiC after deep etching. The morphology of nano-sized TiC particles has a cuboidal shape and their size is about 100 nm. It was reported that the cuboidal TiC particles with (100) facets precipitates in iron melt by



Sample	Position	Composition (at%)			
		Ti	C	Fe	Al
FA-50TiC	1	50.58	41.86	5.15	2.41
	2	38.03	32.25	21.46	8.26
	3	5.82	5.45	65.88	22.84
FA-90TiC	4	48.83	44.74	3.93	2.50
	5	29.79	24.54	38.39	7.28

Fig. 2. SEM micrographs and EDX results of (a) FA-50TiC and (b) FA-90TiC.

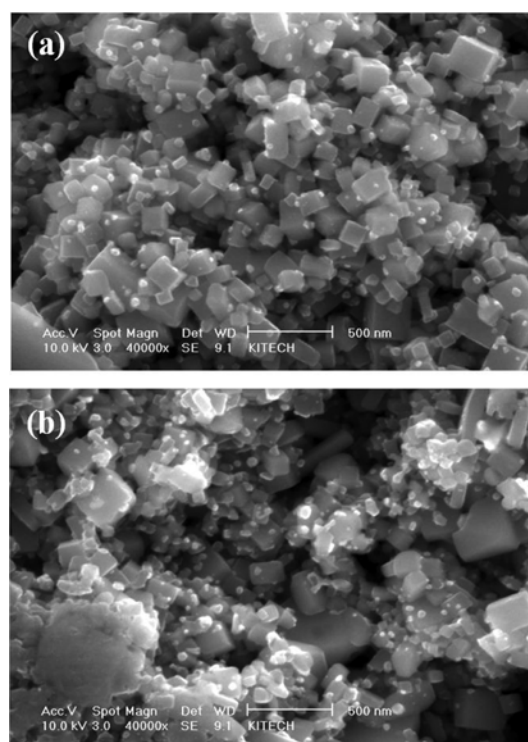


Fig. 3. SEM micrographs of (a) FA-50TiC and (b) FA-90TiC after removing the Fe₃Al binder.

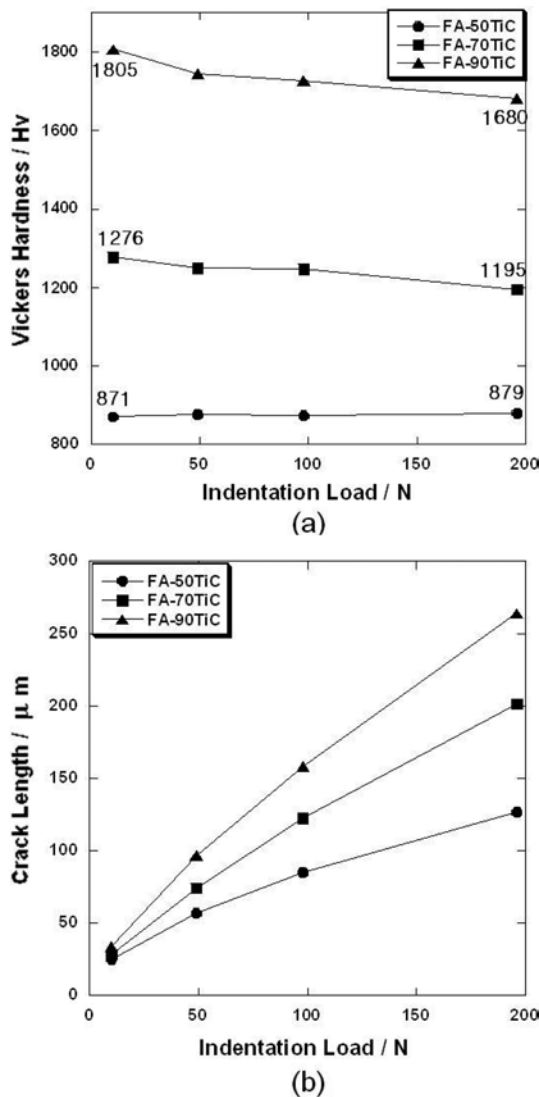


Fig. 4. Effect of indentation load on (a) Vickers hardness and (b) crack length.

in-situ processing with other types of TiC particles such as spherical, starlike and dendritic crystals [14]. On the other hand, the formation of 12-faced polyhedron TiC particles was reported in aluminum melt by an in-situ processing [15]. In previous study [10], the $\text{Fe}_3\text{Al}/\text{TiC}$ composites made by an in-situ melting process also showed the cuboidal shape of TiC particles. The shape of particles produced in in-situ process may be affected by the kind of particle and matrix. Although the formation mechanism of the cuboidal shape of TiC particle is not clear at present, TiC- Fe_3Al system forms the cuboidal shape of TiC regardless of the process manufactured.

Vickers hardness results measured at various indentation loads are shown in Fig. 4. Vickers hardness of the FA-50TiC was unchanged with increasing indentation load, while that of the FA-70TiC and FA-90TiC decreased with increasing load (Fig. 4(a)). However, the crack length increased with increasing indentation load in all samples (Fig. 4(b)). The

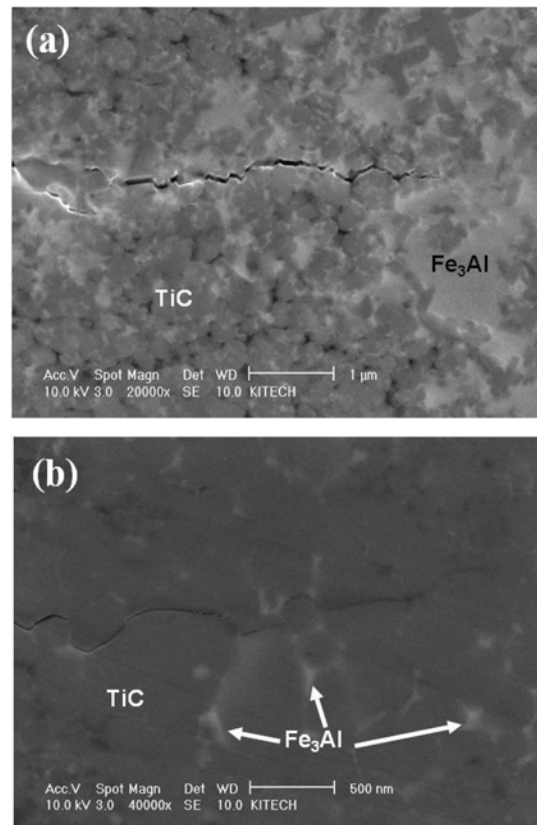


Fig. 5. SEM micrographs of the indentation cracks of (a) FA-50TiC and (b) FA-90TiC.

increasing rate of crack length was different, that is, the crack length of the FA-50TiC increased slowly and that of the FA-90TiC increased rapidly according to increase of indentation load. Therefore, the change of Vickers hardness may relate to the increasing rate of crack length because the crack propagation as well as the formation of indentation mark spends energy. These results can be concluded that the increasing rate of energy spending in the crack propagation increase with the increasing load in the FA-90TiC. On the other hand, the increasing rate of energy spending in crack propagation remains constant in the FA-50TiC regardless of the indentation loads ranged from 9.8 to 196 N. The increasing rate of energy spending in crack propagation may be affected by the toughening effect such as crack deflection and bridging.

The type of crack also can affect the indentation behavior. In general, two types of surface crack are detected in the indentation test of cermets and ceramics: one is the median/radial type and the other is Palmqvist type. The type of crack can be analyzed by fitting the data of crack length to load: one would expect $c \propto P^{2/3}$ for median/radial cracks or $l \propto P^{1/2}$ for Palmqvist cracks, where c is the radius of the surface crack, l is defined as $c-a$, and a is a half-diagonal length of Vickers indent [16, 17]. Analysis of fitting data represented that all samples had the median/radial type relationship of $c \propto P^{2/3}$. As a result, the

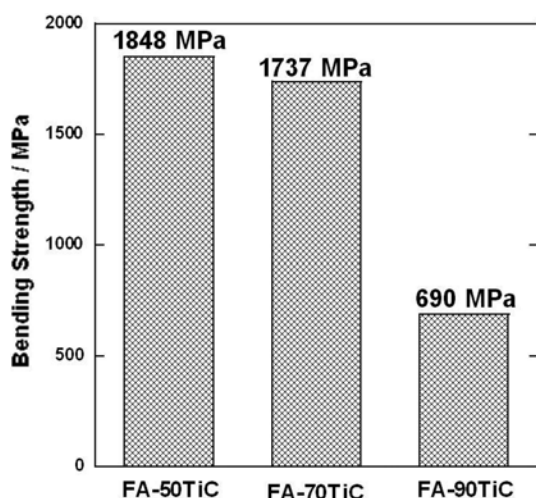


Fig. 6. Bending strength of in-situ cermets.

difference in change of Vickers hardness with the increase of an indentation load is not related to the type of crack.

Fig. 5 shows SEM micrographs exhibiting the crack propagation behavior of the FA-50TiC and FA-90TiC. The crack bridging and crack deflection appeared in all samples. The crack bridging and deflection were dominant in the FA-50TiC and FA-70TiC and crack deflection was prevalent in the FA-90TiC. It is likely that the amounts of toughening in the FA-50TiC and FA-70TiC are larger than that in the FA-90TiC. The change of toughening mechanism may relate to the volume fraction of the Fe_3Al phase.

The effect of TiC volume fraction on the bending strength is illustrated in Fig. 6. As volume fraction of TiC increased, the bending strength decreased. Although the FA-50TiC and FA-70TiC maintained relatively high bending strength above 1700 MPa, the strength of the FA-90TiC was rapidly dropped. This result can be accounted for the role of Fe_3Al phase on toughing of cermets. The indentation results indicate that Fe_3Al phase was effective on the prevention of crack propagation. Also, the decrease of the strength and fracture toughness with the decrease of amounts of binder phase was reported in other types of cermets. Therefore, it can be concluded that certain amounts of Fe_3Al phase are necessary to maintain the strength of cermets. In addition, it may also be a reason of the lower strength that the FA-90TiC has relative density lower than other cermets.

Conclusions

TiC/Fe-28 at%Al cermets with TiC of 50-90 vol% were made by in-situ reaction during mechanical alloying and sintering. During milling process, mechanical alloying promoted the formation of TiC and the solid solution of Fe and Al into TiC. The synthesis of TiC and Fe_3Al was completed during sintering and the relative densities of sintered bodies were above 95%. The microstructures of cermets with TiC of 50 and 70 vol% consisted of micro-sized TiC particles, nano-sized TiC particles with Fe_3Al binder and TiC-free Fe_3Al region, while that with 90 vol% TiC showed TiC and Fe_3Al regions. It was found that the binder phase, Fe_3Al , was effective on the prevention of crack propagation in cermets with 50 ~ 70 vol % TiC. The bending strength of cermets with 50 ~ 70 vol % TiC was above 1700 MPa.

References

1. C.T. Liu, MRS symposium proceedings (1993) 3-19.
2. C.G. Mckamey, J.H. Devan, P.F. Tortorelli and V.K. Sikka, *J. Mater. Res.* 6 (1991) 1779-1805.
3. S.H. Ko, R. Gnanamoorthy and S. Hanada, *Mater. Sci. Eng. A222* (1997) 133-139.
4. J.H. Schneibel, C.A. Carmichael, E.D. Specht and R. Subramanian, *Intermetallics* 5 (1997) 61-67.
5. R. Subramanian and J.H. Schneibel, *JOM* 49 (1997) 50-54.
6. M.X. Gad, F.J. Oliveira, Y. Pan, L. Yang, J.L. Baptista and J.M. Vieira, *Intermetallics* 13 (2005) 460-466.
7. R. Subramanian and J.H. Schneibel, *Mater. Sci. Eng. A244* (1998) 103-113.
8. R. Subramanian and J.H. Schneibe, K.B. Alexander and K.P. Plucknett, *Scripta Mater.* 35 (1996) 583-588.
9. B.S. Murty and S. Ranganathan, *Int. Mater. Rev.* 43 (1998) 101.
10. S.H. Ko and S. Hanada, *Intermetallics* 7 (1999) 947-955.
11. S.H. Ko, B.G. Park, H. Hashimoto, T. Abe and Y.H. Park, *Mater. Sci. Eng. A329-331* (2002) 78-83.
12. M.S. El-Eskandarany, T.J. Konno, K. Sumiyama and K. Suzuki, *Mater. Sci. Eng. A217/218* (1996) 265-268.
13. P. Matteazzi, G.L. Caer and A. Mocellin, *Ceram. Inter.* 23 (1997) 39-44.
14. Z. Liu and H. Fredriksson, *Metall. Mater. Trans.* 28A (1997) 471-483.
15. H. Morimoto, M. Nomura and Y. Ashida, *J. Japan Inst. Metals* 59 (1995) 429-436.
16. J.D. Lin and J.G. Duh, *Mater. Chem. & Phys.* 78 (2002) 253-261.
17. C.C. Anya and S.G. Roberts, *J. Eur. Ceram. Soc.* 16 (1996) 1107-1114.